



### Keywords

Silicon,  
Transition Metals,  
Simulation,  
Gettering Optimization

Received: March 8, 2017

Accepted: March 31, 2017

Published: June 7, 2017

# Simulation of Multi-Plateau-Temperature Process Intended for Simultaneous Gettering of Chromium, Iron and Nickel in Silicon

Nabil Khelifati<sup>1, 2, \*</sup>, Djoudi Bouhafs<sup>1</sup>, Seddik-El-Hak Abaidia<sup>2</sup>, Yacine Kouhlane<sup>1</sup>

<sup>1</sup>Division of Development of Semiconductor Conversion Devices, Research Center in Semiconductor Technology for the Energetic (CRTSE / ex. UDTS), Algiers, Algeria

<sup>2</sup>Department of Physics, Faculty of Sciences, M'hamed Bougara University of Boumerdès (UMBB), Boumerdès, Algeria

### Email address

n.khelifati@gmail.com (N. Khelifati)

\*Corresponding author

### Citation

Nabil Khelifati, Djoudi Bouhafs, Seddik-El-Hak Abaidia, Yacine Kouhlane. Simulation of Multi-Plateau-Temperature Process Intended for Simultaneous Gettering of Chromium, Iron and Nickel in Silicon. *Journal of Materials Sciences and Applications*. Vol. 3, No. 1, 2017, pp. 8-13.

### Abstract

In this paper, computational results of simultaneous gettering of chromium (Cr), iron (Fe) and nickel (Ni) in p-type silicon by phosphorus diffusion are presented. The study was carried out by a software tool "GetProg" developed in our centre CRTSE. Simulated aspect includes impurity diffusion, segregation and also precipitates dissolution phenomenon. The kinetics of dissolved impurities gettering has been described by a diffusion-segregation equation (DSE) extended by precipitates dissolution term. The input initial parameters of metals in material were mainly taken from experimental results obtained for sheet multicrystalline silicon. The simulation allowed the study of the simultaneous behaviour of Cr, Fe and Ni during an optimized multi-plateau-gettering process (MPG). Two MPG scenarios have been investigated; High-Low and Low-High temperature. The findings demonstrate that the MPG effectiveness of studied metals depends significantly on the nature of metal and its initial concentration, as well as the used MPG scenario.

## 1. Introduction

Both upgraded-metallurgical grade (UGM) and solar grade (SoG) silicon destined to solar cells fabrication contain various kinds of metal impurities such as Cr, Fe, Ni and Cu, with concentrations vary generally between  $10^{12} \text{ cm}^{-3}$  and  $10^{17} \text{ cm}^{-3}$ . The presence of such impurities in the material create deep level states in band gap, and generate lifetime killing recombination centers and junction leakage currents [1-4]. Consequently, an important degradation in the efficiency potential of solar cells will be seen [5, 6].

Nevertheless, most metallic impurities dissolved or precipitated can be more or less removed from the bulk of material, using extrinsic gettering technique. It refers to a thermal process step that dissolves the metallic precipitates and activates the diffusion of dissolved metals from the bulk to a high solubility surface region. This later can be generally created by phosphorus diffusion ( $n^+$ ), boron diffusion ( $p^+$ ), and / or by aluminium-silicon (Al-Si) alloying [7-15].

Currently, the most well studied metal contaminant in silicon is iron (Fe), and this is due to its obvious high lifetime-killing effect. Beside experimental works, different kinetics process simulation tools have been developed to engineer its distribution and investigate its behaviour in the material during gettering process [16-19]. Chromium (Cr) is also a well-known detrimental impurity in silicon, impacting silicon based solar cells performance even at concentrations as low as  $10^{10} \text{ cm}^{-3}$  [20-22]. Its acceptable total concentration in a p-type silicon wafer is around  $10^{13} \text{ cm}^{-3}$ , which is lower by one order of magnitude comparing to iron [23]. Furthermore, the harmful effect of Cr in silicon can be especially observed in its interstitial state ( $\text{Cr}_i$ ), where the capture cross-sections are 1.5 and 57 times larger than iron in p- and n-type silicon, respectively [21].

Like iron and chromium, nickel is one of the more thoroughly investigated contaminant metals. It is known to be a fast diffuser with high solubility in Si. In spite of intensive research made on this metal, its electrical properties are poorly understood and the existing data on its energy levels and its recombination activity are still controversial [24]. The fraction of electrically active Ni in Si is about 1% of the respective solubility, with a mid-band gap energy level at  $E_c-0.4\text{eV}$  and  $\sigma_n = 5.6 \times 10^{-17} \text{ cm}^2$  (case of p-type Si) [25]. Its majority carrier capture cross section was found to be in the range  $10^{-16} - 10^{-17} \text{ cm}^2$  both in p- and n-type silicon [26, 27].

Despite the detrimental effects of chromium and nickel in Si, they have not sufficiently investigated as much as iron, especially, during processing steps. Moreover, the majority of published works dealing with this subject metal by metal and separately.

In this paper, we investigated by simulation, using our software tool "GetProg", the feasibility of simultaneous segregation gettering of chromium, iron and nickel in p-type silicon. The effectiveness of High-Low and Low-High multi-plateau-gettering processes (MPG) has been studied and evaluated through the fundamental electron lifetime. This study is the perspective of our work previously presented [28].

## 2. Simulation

The model used for the simulation describes the variation of interstitial impurity concentration  $C_i$  as a function of the depth, the time and also the gettering process temperature. It refers to a space-time differential equation that quantifies the segregation and the dissolution of precipitates phenomenon. The kinetics of gettered impurity is described by a diffusion segregation equation (DSE) [29] extended by an additional term which describes the dissolution of impurity precipitates [30], as shown in equation (1) below

$$\frac{\partial C_i}{\partial t} = \frac{\partial}{\partial x} \left[ D \left( \frac{\partial C_i}{\partial x} - \frac{C_i}{m} \frac{\partial m}{\partial x} \right) \right] + 4\pi D N_p r_p (C_{eq} - C_i) \quad (1)$$

The first term, introduced by Tan et al. [31], gives the

evolution of dissolved impurity concentration in the bulk ( $C_i$ ) having the diffusivity  $D$  and the segregation coefficient  $m$ . The second term known as Ham's law [32] represents the dissolution of precipitated impurity atoms with a precipitate density  $N_p$  and a radius  $r_p$ .  $C_{eq}$  is the solid solubility of dissolved metallic impurity in silicon. The segregation coefficient used in our simulation describes the metal segregation into phosphorus diffusion region rich in phosphorus-vacancy complex ( $\text{P}_4\text{V}$ ). It can be given by the following formula [8]:

$$m(\text{P}_4\text{V}) = 1 + K_{\text{P}_4\text{V}} [\text{P}_4\text{V}] \quad (2)$$

where  $K_{\text{P}_4\text{V}}$  is an equilibrium constant related to the formation energy ( $E_b$ ) of  $\text{M-P}_4\text{V}$  clusters. The values of formation energy of Cr-, Fe- and Ni- $\text{P}_4\text{V}$  used in this study are 1.99 eV, 1.52 eV and 1.92 eV, respectively [33].

More details on the segregation coefficient, diffusivity, solid solubility and as well as the approximation done to simplify the calculation can be found in Ref. [30-36].

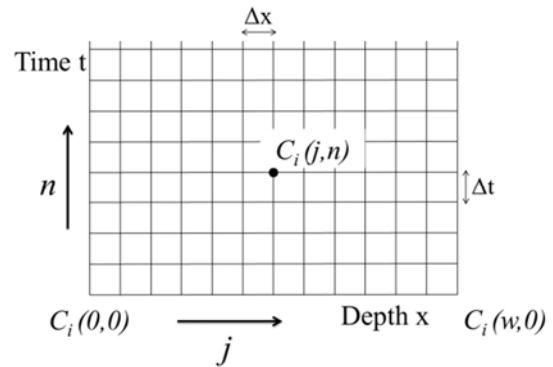


Figure 1. Finite element mesh platform used in the simulation.

Using the finite element mesh platform shown in Figure 1, a numerical resolution of equation (1) led to follow the variation of dissolved metal concentration  $C_i(x, t)$  as a function of the depth  $x$ , time  $t$  and temperature  $T$  of the gettering process. Assuming that the initial dissolved metal concentration  $C_{i0}=C_i(x, 0)$  is uniformly distributed along the silicon wafer thickness, the initial and boundary conditions used in the resolution of equation (1) can be, respectively, given as following

Initial condition:

$$C_i(x, t = 0) = C_{i0} \quad (3)$$

Boundary conditions:

$$\begin{cases} m \frac{\partial C_i(x=0,t)}{\partial t} = D \frac{\partial C_i(x=0,t)}{\partial x} \\ D \frac{\partial C_i(x=w,t)}{\partial x} = 0 \end{cases} \quad (4)$$

The approach used in this simulation is based on an explicit method, which is conditionally stable verifying equation (5). Therefore, the choice of adequate space-time parameters is indispensable to perform a stable simulation with reduced error.

$$D \frac{\Delta t}{(\Delta x)^2} \leq \frac{1}{2} \quad (5)$$

### 3. Results and Discussion

In our previous study [28], we have compared the influence of annealing temperature on the gettering effectiveness of Cr and Fe in silicon separately and without taking into account the effect of optimized gettering temperature ( $T_{opt}$ ) of each metal on the concentration of other. In this present investigation, we assume that the material is simultaneously contaminated by Cr, Fe and Ni at different levels. The total initial chromium, iron and nickel concentrations were taken equal to  $1.2 \times 10^{15} \text{ cm}^{-3}$ ,  $1.4 \times 10^{16} \text{ cm}^{-3}$  and  $4.2 \times 10^{15} \text{ cm}^{-3}$ , with associated initial precipitate radii of 30 nm, 50 nm and 40 nm, respectively. These concentrations cover the most usual contamination level

found in sheet multicrystalline silicon [37]. The as-grown interstitial concentrations are assumed to be  $5 \times 10^{12} \text{ cm}^{-3}$  for all the metallic impurities.

Because each metal can be effectively gettered only at a specified optimum temperature  $T_{opt}$ , it's clear that the simultaneous presence of these three metals in material requires a multi-plateau-gettering (MPG) process of three annealing stages. The temperature  $T_{opt}$  of each plateau corresponding to a given metal can be more or less influenced by the previous one. Indeed, simulation results illustrated in figure 2 (open symbols) demonstrate that an effective gettering of Ni, Fe and Cr can be only done at temperature ranges; 200-400°C, 400-700°C and 625-775°C, respectively. So, one can note that there is various scenarios to perform a process MPG regarding the first impurity to be gettered.

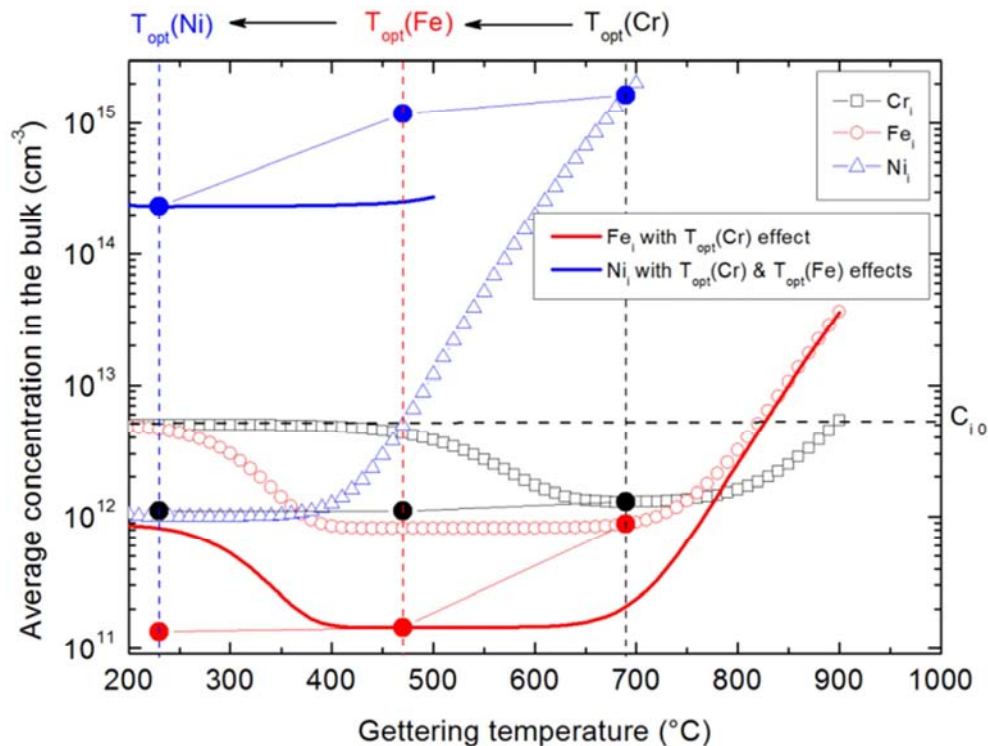


**Figure 2.** Evolution of the average concentrations of chromium, iron and nickel in the bulk as function of temperature for High-Low temperature process.

In the following, we tested by simulation the effectiveness of High-Low and Low-High MPG scenarios during an extended time of 120 minutes. The first one starts by the gettering of Cr at  $T_{opt}(Cr)$  situated around 690°C, followed by that of Fe at  $T_{opt}(Fe)$  varies typically in the range 400-600°C. This scenario finishes by low temperature ramp  $T_{opt}(Ni)$  varies between 200°C and 400°C. In the second scenario (e. g. Low-High), the simulation starts by gettering plateau of Ni and terminates by that of Cr at high temperature. It's important to note that the effect of each plateau on the concentration of the metals and their optimized gettering temperatures have been taken into account.

Figure 3 shows the evolution of average concentrations of interstitial metals in the bulk as function of temperature for

High-Low scenario process. The curves in open symbols represent the independent variation of content of each metal, while the curves in lines and closed symbols represent the concentrations variation after different anneal plateaus. In this scenario, the annealing at  $T_{opt}(Cr)=690^\circ\text{C}$  / 120 min decreases  $[Cr_i]$  from  $5 \times 10^{12} \text{ cm}^{-3}$  to  $1.3 \times 10^{12} \text{ cm}^{-3}$ . The effect of this process step on iron and nickel concentrations is notable. Indeed, after this annealing  $[Fe_i]$  decreases considerably from its initial value to  $8.84 \times 10^{11} \text{ cm}^{-3}$  indicating a reduction of about 82% of interstitial iron in the material bulk, while  $[Ni_i]$  increases to a very high concentration ( $1.64 \times 10^{15} \text{ cm}^{-3}$ ) which is equal to the limit solubility of nickel in Si at 690°C. This rapid increment of  $[Ni_i]$  is due to the dissolution of Ni-Si precipitates during annealing.

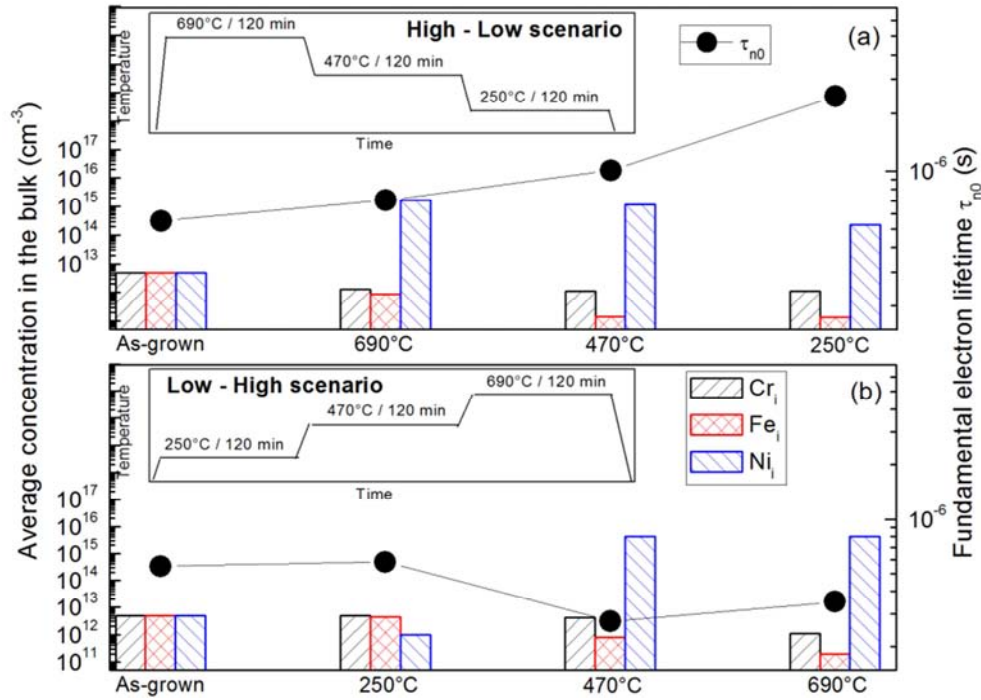


**Figure 3.** Variation of the average concentrations of chromium, iron and nickel (coloured bars) and the associated fundamental electron lifetime  $\tau_{n0}$  (black symbols) as function of optimized gettering temperature for High-Low (a) and Low-High (b) scenarios.

Taking these concentrations as new initial parameters to use them in the second plateau, the optimum gettering temperature of iron is calculated to be  $T_{opt}(Fe)=470^{\circ}C$  with  $[Fe_i]=1.45 \times 10^{11} \text{ cm}^{-3}$  (see red line curve).  $[Ni_i]$  decreases slightly and an additional decreasing of Cr content has been observed. The third annealing plateau associated to Ni impurity yields a notable diminution of  $[Ni_i]$  from  $1.18 \times 10^{15} \text{ cm}^{-3}$  to  $2.34 \times 10^{14} \text{ cm}^{-3}$ , accompanied by a constancy of  $[Cr_i]$  and  $[Fe_i]$ . The final concentrations of  $Cr_i$ ,  $Fe_i$  and  $Ni_i$  in the bulk are respectively;  $1.11 \times 10^{12} \text{ cm}^{-3}$ ,  $1.34 \times 10^{11} \text{ cm}^{-3}$  and  $2.34 \times 10^{14} \text{ cm}^{-3}$ .

The same simulation is done for Low-High scenario and the findings were compared with those of High-Low scenario discussed above, as shown in figures 3 (a) and (b). Based on this variety of results, one can remark that there is a competition between beneficial and detrimental effects which can be, respectively, observed through the increasing and decreasing of interstitial metal concentration. For both scenarios, all annealing plateaus reduce progressively the iron and chromium content in the bulk indicating an effective gettering, while increase the concentration of interstitial nickel to high level due to the dissolution of Ni-silicide precipitates.

Because of the different carrier capture cross sections of the studied metals, the investigation of electrical propriety of material during the MPG process using only the evolution of metals concentrations is not adequate. So, the investigation can be made by the monitoring of the fundamental electron lifetime  $\tau_{n0}$ . This parameter is determined throughout the wafer thickness by Shockley-Read-Hall statistics as following [38]:

$$\frac{1}{\tau_{n0}} = v_{th} \sum_i C_i \sigma_{ni} \quad (6)$$

where  $v_{th}$  is the thermal velocity of electron,  $C_i$  and  $\sigma_{ni}$  are the concentration of interstitial impurity and the electron capture cross section, respectively.

Based on equation (6) and using the metals concentrations obtained by simulation, the variation of  $\tau_{n0}$  for each scenario is calculated and presented in figures 3 (a) and (b). It is clear that the first scenario yields a progressive improvement of the electron lifetime, while the second one deteriorates it especially at annealing plateaus correspond to iron and chromium gettering. These results demonstrate that a simultaneous gettering of chromium, iron and nickel can be effectively done by series of specified annealing plateaus vary from high to low temperature (e.g. High-Low scenario).

## 4. Conclusion

Simultaneous gettering of Cr, Fe and Ni in silicon is investigated by simulation. Two multi-plateau-gettering process (MPG) scenarios were used; High-Low and Low-High temperature. The findings demonstrate that the MPG effectiveness of the three impurities together depends significantly on the nature of metals and their initial concentrations, as well as the MPG scenario. High-Low scenario shows a notable improvement in electron lifetime due to effective gettering, while Low-High scenario yields lifetime degradation which is mainly due to the Ni silicide dissolution at high temperatures.

## Acknowledgements

This work has been supported by the General Directorate for Scientific Research and Technological Development (Direction Générale de la Recherche Scientifique et du Développement Technologique, DGRSDT / Algeria).

## References

- [1] K. Graff, *Metal Impurities in Silicon Device Fabrication*, Springer-Verlag, Berlin, Germany (1994), p. 13; DOI: 10.1007/978-3-642-97593-6.
- [2] E. R. Weber and D. Gilles, *Semiconductor silicon* (1990), H. R. Hu, K. G. Barraclough and J. Chikawa, Eds., PV 90-7, p. 585, The Electrochem. Soc. Proc. Series, Pennington, NJ (1990).
- [3] W. Bergholz, G. Zoth, F. Gelsdorf and B. Kolbeson, *Defects in Silicon II*, (1991).
- [4] W. M. Bullis, U. Gosele and F. Shimura, Eds., PV 91-9, p. 21, The Electrochem. Soc. Proc. Series, Pennington, NJ (1991).
- [5] A. Istratov, T. Buonassisi, R. J. McDonald, A. Smith, R. Schindler, J. Rand, J. Kalejs, E. R. Weber, Metal content of multicrystalline silicon for solar cells and its impact on minority carrier diffusion length, *J. Appl. Phys.* 94, (2003) 6552; <http://dx.doi.org/10.1063/1.1618912>.
- [6] A. Laades, K. Lauer, M. Bähr, C. Maier, A. Lawerenz, D. Alber, J. Nutsch, J. Lossen, C. Koitzsch, R. Kibizov, Impact of Iron Contamination on CZ-Silicon Solar Cells, *Proceedings of 23<sup>rd</sup> European Photovoltaic Solar Energy Conference*, Valencia, Spain (2008); doi: 10.4229/23rdEUPVSEC2008-2CV.5.46.
- [7] S. P. Phang and D. Macdonald, Direct comparison of boron, phosphorus, and aluminum gettering of iron in crystalline silicon, *J. Appl. Phys.* 109, (2011) 073521; <http://dx.doi.org/10.1063/1.3569890>.
- [8] J. Schön, V. Vähänissi, A. Haarahiltunen, M. C. Schubert, W. Warta and H. Savin, Main defect reactions behind phosphorus diffusion gettering of iron, *J. Appl. Phys.* 116, (2014) 244503; <http://dx.doi.org/10.1063/1.4904961>.
- [9] J. Schön, M. C. Schubert, W. Warta, H. Savin, and A. Haarahiltunen, Analysis of simultaneous boron and phosphorus diffusion gettering in silicon, *Phys. Status Solidi A* 207, No. 11, (2010) 2589 - 2592; DOI: 10.1002/pssa.201026333.
- [10] A. Haarahiltunen, H. Talvitie, H. Savin, M. Yli-Koski, M. I. Asghar, and J. Sinkkonen, Modeling boron diffusion gettering of iron in silicon solar cells, *Appl. Phys. Lett.* 92, (2008) 021902; <http://dx.doi.org/10.1063/1.2833698>.
- [11] A. Ben Jaballah, M. Hassen, H. Rahmouni, M. Hajji, A. Selmi, H. Ezzaouia, Impacts of phosphorus and aluminum gettering with porous silicon damage for p-type Czochralski silicon used in solar cells technology, *Thin Solid Films* 511–512 (2006) 377–380; <http://dx.doi.org/10.1016/j.tsf.2005.11.101>.
- [12] I. Perichaud, Gettering of impurities in solar silicon, *Solar Energy Materials & Solar Cells* 72 (2002) 315–326; [http://dx.doi.org/10.1016/S0927-0248\(01\)00179-9](http://dx.doi.org/10.1016/S0927-0248(01)00179-9).
- [13] P. S. Plekhanov, M. D. Negoita, and T. Y. Tan, Effect of Al-induced gettering and back surface field on the efficiency of Si solar cells, *J. Appl. Phys.* 90, (2001) 5388; <http://dx.doi.org/10.1063/1.1412575>.
- [14] V. Kveder, W. Schröter, A. Sattler, M. Seibt, Simulation of Al and phosphorus diffusion gettering in Si, *Materials Science and Engineering B71* (2000) 175–181; [http://dx.doi.org/10.1016/S0921-5107\(99\)00370-0](http://dx.doi.org/10.1016/S0921-5107(99)00370-0).
- [15] M. Loghmarti, R. Stuck, J. C. Muller, D. Sayah, and P. Siffert, Strong improvement of diffusion length by phosphorus and aluminum gettering, *Appl. Phys. Lett.* 62, (1993) 979; <http://dx.doi.org/10.1063/1.108539>.
- [16] C. del Canizo and A. Luque, A Comprehensive model for the gettering of lifetime-killing impurities in silicon, *J. Electrochem. Soc.* 147 (7) (2000) 2685-2692; doi: 10.1149/1.1393590.
- [17] A. Haarahiltunen, H. Savin, M. Yli-Koski, H. Talvitie, and J. Sinkkonen, Modeling phosphorus diffusion gettering of iron in single crystal silicon, *J. Appl. Phys.* 105, (2009) 023510; <http://dx.doi.org/10.1063/1.3068337>.
- [18] J. Hofstetter, D. P. Fenning, M. I. Bertoni, J. F. Lelièvre, C. del Canizo, and T. Buonassisi, Impurity-to-efficiency simulator: predictive simulation of silicon solar cell performance based on iron content and distribution, *Prog. Photovolt: Res. Appl.*, 19: 487–497; doi: 10.1002/pip.1062.
- [19] D. P. Fenning, A. S. Zuschlag, J. Hofstetter, A. Frey, M. I. Bertoni, G. Hahn, and T. Buonassisi, Investigation of lifetime-limiting defects after high-temperature phosphorus diffusion in highiron-content multicrystalline silicon, *IEEE J. Photovoltaics*, vol. 4, no. 3 (2014) 866 - 873; doi: 10.1109/JPHOTOV.2014.2312485.
- [20] J. R. Davis, A. Rohatgi, R. H. Hopkins, P. D. Blais, P. Rai-Choudhury, J. R. McCormick, and H. C. Mollenkopf, *Impurities in silicon solar cells*, no. 4, 1980.
- [21] J. Schmidt, B. Lim, D. Walter, K. Bothe, S. Gatz, T. Dullweber, and P. P. Altermatt, “Impurity related limitations of next-generation industrial silicon solar cells,” *IEEE J. Photovoltaics*, vol. 3, no. 1 (2013) 114 - 118; doi: 10.1109/JPHOTOV.2012.2210030.
- [22] G. Coletti, Sensitivity of state-of-the-art and high efficiency crystalline silicon solar cells to metal impurities, *Prog. Photovolt: Res. Appl.*, vol. 21, no. 5 (2013) 1163–1170; doi: 10.1002/pip.2195.
- [23] J. Hofstetter, J. F. Lelièvre, C. del Canizo, A. Luque, Acceptable contamination levels in solar grade silicon: From feedstock to solar cell, *Materials Science and Engineering B* 159–160, 299–304 (2009); <http://dx.doi.org/10.1016/j.mseb.2008.05.021>.
- [24] A. A. Istratov, E. R. Weber, Electrical properties and recombination activity of copper, nickel and cobalt in silicon, *Appl. Phys. A* 66, 123–136 (1998); doi: 10.1007/s003390050649.
- [25] S. Rein, *Lifetime Spectroscopy*. Berlin, Germany, Springer (2005); DOI: 10.1007/3-540-27922-9.
- [26] H. Kitagawa, S. Tanaka, H. Nakashima, M. Yoshida, Electrical properties of nickel in silicon, *J. Electron. Mater.* 20, (1991) 441; doi: 10.1007/BF02657824.

- [27] W. B. Chua, K. Rose, Electrical Properties of High-Resistivity Nickel-Doped Silicon, *J. Appl. Phys.* 41 (1970) 2644; <http://dx.doi.org/10.1063/1.1659275>.
- [28] N. Khelifati, D. Bouhafis, S-E-H. Abaidia, A. Boucheham and B. Palahouane, Proceedings of 29<sup>th</sup> European Photovoltaic Solar Energy Conference and Exhibition, Amsterdam, Netherlands (2014).
- [29] T. Y. Tan, Mass transport equations unifying descriptions of isothermal diffusion, thermomigration, segregation, and position-dependent diffusivity, *Appl. Phys. Lett.* 73 (1998) 2678; <http://dx.doi.org/10.1063/1.122551>.
- [30] P. S. Plekhanov, R. Gafiteanu, U. M. Gösele, T. Y. Tan, Modeling of gettering of precipitated impurities from Si for carrier lifetime improvement in solar cell applications, *J. Appl. Phys.* 86, 2453 (1999); <http://dx.doi.org/10.1063/1.371075>.
- [31] T. Y. Tan, R. Gafiteanu, S. M. Joshi, and U. Gösele, "Science and Modeling of Impurity Gettering in Silicon", in *Semiconductor Silicon 1998*, eds. H. R. Huff, U. Gösele, and H. Tsuya (The Electrochem. Soc., Pennington, NJ, 1998) p. 1050.
- [32] F. Ham, Theory of diffusion limited precipitation, *J. Phys. Chem. Solids* 6 (1958) 335; doi: 10.1016/0022-3697(58)90053-2.
- [33] R. Chen, B. Trzynadlowski, and S. T. Dunham, Phosphorus vacancy cluster model for phosphorus diffusion gettering of metals in Si, *J. Appl. Phys.* 115, (2014) 054906; <http://dx.doi.org/10.1063/1.4864377>.
- [34] K. Lauer, A. Laades, A. Lawrenz, K. Neckermann, A. Sidelnicov, Impact of Different Annealing Steps on the Interstitial Iron Concentration in Solar-Grade Czochralski Silicon, Proceedings of 25<sup>th</sup> European Photovoltaic Solar Energy Conference and Exhibition, Valencia, Spain (2010); 10.4229/25thEUPVSEC2010-2CV.3.76.
- [35] M. Blazek, W. Kwapil, J. Schön and W. Warta, Gettering Efficiency of Backside Aluminium Layer and Al-Si-Eutectic, Proceedings of 23<sup>rd</sup> European Photovoltaic Solar Energy Conference, Valencia, Spain (2008); doi: 10.4229/23rdEUPVSEC2008-2CV.5.16.
- [36] T. Y. Tan, Subcontract Report, NREL / SR-520-37991 (2005).
- [37] T. Buonassisi, A. A. Istratov, M. D. Pickett, M. Heuer, J. P. Kalejs, G. Hahn, M. A. Marcus, B. Lai, Z. Cai, S. M. Heald, T. F. Ciszek, R. F. Clark, D. W. Cunningham, A. M. Gabor, R. Jonczyk, S. Narayanan, E. Sauar, E. R. Weber, Chemical natures and distributions of metal impurities in multicrystalline silicon materials, *Prog. Photovolt: Res. Appl.*, 14 (2006) 513-531; doi: 10.1002/pip.690.
- [38] J. Nelson, *The Physics of Solar Cells*, Imperial College Press (2003).